ACS APPLIED MATERIALS & INTERFACES

Research Article

www.acsami.org

Novel Multifunctional Hybrids of Single-Walled Carbon Nanotubes with Nucleic Acids: Synthesis and Interactions with Living Cells

Evgeny K. Apartsin,*[,†] Marina Yu. Buyanova,[†,‡] Darya S. Novopashina,[†] Elena I. Ryabchikova,[†] Anton V. Filatov,[†] Marina A. Zenkova,[†] and Alya G. Venyaminova[†]

[†]Institute of Chemical Biology and Fundamental Medicine SB RAS, 8 Lavrentiev Avenue, Novosibirsk 630090, Russian Federation

[‡]Novosibirsk State University, 2 Pirogov str., Novosibirsk 630090, Russian Federation

Supporting Information

ABSTRACT: Novel hybrids of fluorescein-labeled poly(ethylene glycol)-modified single-walled carbon nanotubes (SWCNTs) with nucleic acids were prepared. 5′-Pyrene conjugates of oligodeoxyribonucleotides were used to construct the noncovalent hybrids, with the pyrene residues acting as anchor groups, immobilizing an oligonucleotide on the SWCNT surface. The hybrid formation characteristics were studied using ζ-potential measurements and adsorption isotherm plots. Transmission electron microscopy (TEM) of the samples stained with contrast agents proved that the pyrene conjugates of oligonucleotides were adsorbed onto the surfaces of the functionalized SWCNTs. On the basis of the MTT assay, the functionalized SWCNTs and their hybrids with oligonucleotides exhibited low toxicity toward HeLa, KB-3-1, and KB-8-5 cells. A TEM study of ultrathin sections of cells treated with SWCNTs revealed that the nanotubes directly interacted with the cellular surface.

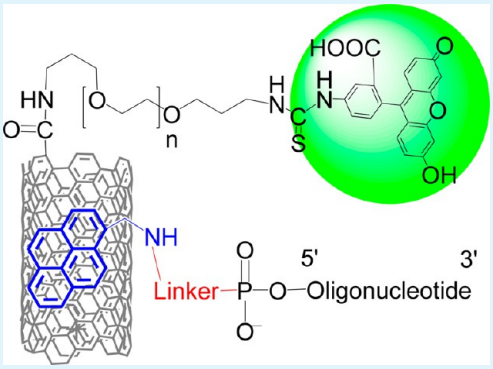

KEYWORDS: *carbon nanotubes, PEGylation, oligonucleotides, pyrene, hybrids, MTT assay*

1. INTRODUCTION

Carbon nanotubes (CNTs) have unique chemical and physical properties and, when functionalized, are compatible with biomacromolecules and cells. Modern synthetic methods make possible the chemical functionalization of CNTs containing organic, inorganic, and heteroorganic fragments.[1,2] Hybrids of CNTs with nucleic acids, proteins, and other biological molecules have wide-ranging applications. CNT–nucleic acid hybrids are used in target-molecule detection systems[3] and in nanomedicine as transporters of therapeutic nucleic acids.[4−6] CNTs may be applied as intracellular nucleic acid transporters because of both their ability for highly efficient cellular penetration[7] and low toxicity when modified with hydrophilic molecules.[5,8] PEGylation [the attachment of poly(ethylene glycol) (PEG)] was reported as a powerful method for increasing the hydrophilicity of single-walled carbon nanotubes (SWCNTs), thereby increasing their solubility and biocompatibility.[9,10] In addition, SWCNT-based hybrid constructs should contain reporter groups to allow monitoring of their penetration through the cell membrane, intracellular distribution after transfection, and withdrawal from the cells by means of confocal microscopy.[11]

To date, various methods have been proposed for attaching nucleic acids to the SWCNT surface, both covalently and noncovalently.[12] The use of anchor groups or the noncovalent immobilization of oligonucleotides on the SWCNT surface is promising, with a diaminopoly(ethylene glycol)–phospholipid conjugate being one of them. Upon functionalization, lipid tails cover the CNT surface, and PEG brings the high solubility to the whole construction. Terminal amino groups are available for conjugation with oligonucleotides.[13−16]

Another powerful approach for immobilizing nucleic acids on CNTs involves pyrene anchor groups that interact with the CNT surface through strong π–π-stacking interactions.[12,17−19] This method is promising because of the relative simplicity of synthesizing pyrene conjugates of oligonucleotides and the high density of CNT functionalization by pyrene. We developed this method by combining the noncovalent anchoring of oligonucleotides on the CNT surface and the PEGylation of the CNT tips and defective sites to form multifunctional hybrids. This combination of methods permitted the separate functionalization of both types of CNT reactive sites (the tips and defective sites and the defect-free surface), enabling their efficient use (as previously demonstrated for the covalent functionalization of both types of sites[20]). Covalent attachment of PEG moieties on the SWCNT surface increases the potential biocompatibility of the hybrids formed using these SWCNTs,[9,10] and the noncovalently immobilized oligonucleotide can be released from the SWCNT surface inside a cell. The release can be achieved due to hydrolysis of the pyrene–

Received: August 19, 2013
Accepted: January 3, 2014
Published: January 3, 2014

oligonucleotide bond in acidic media in lysosomes,[21] displacement of anchored oligonucleotides from the SWCNT surface,[22] or spontaneous decomposition of the hybrid.[23]

We report the preparation of noncovalent hybrids of pyrene-modified oligonucleotides with fluorescently labeled PEGylated SWCNTs and the study of their interactions with living cells.

2. MATERIALS AND METHODS

2.1. Materials. SWCNT-COOH (500−1500 nm in length, Aldrich, St. Louis, MO) was used as a platform for constructing multifunctional hybrids. Oligodeoxyribonucleotides were synthesized using the solid-phase phosphoramidite method on an ASM-800 automated synthesizer (Biosset, Novosibirsk, Russia). 5′-Terminal hexa(ethylene glycol) phosphate or 5′-terminal phosphate groups were introduced into the oligonucleotides during the final stages of the synthesis via condensation of the polymer-bound protected oligonucleotide with the H-phosphonates of *O*-(4,4′-dimethoxytrityl)-hexakis(ethylene glycol) and/or [2-[2-(4,4′-dimethoxytrityloxy)ethyl]-sulfonyl]ethanol using pivaloyl chloride as the activator. The H-phosphonates were synthesized as previously described.[24]

2.2. Cell Lines. Two lines of human cervical carcinoma cells (HeLa and KB-3-1) were obtained from the Institute of Cytology RAS (St. Petersburg, Russia). KB-8-5 cells with a multidrug-resistance phenotype derived from KB-3-1 cells were kindly provided by Prof. M. Gottesmann (NIH, Bethesda, MD). The cell lines were maintained in Dulbecco's modified eagle medium (DMEM; Gibco) supplemented with 10% fetal bovine serum (FBS), 100 U/mL of penicillin, 100 mg/L of streptomycin, and 0.25 mg/L of amphotericin under a humidified atmosphere containing 5% CO_2/95% air at 37 °C. The medium for culturing the KB-8-5 cells was supplemented with vinblastine (300 mg/L).

2.3. Instrumentation. IR spectra of the functionalized SWCNTs were recorded using a Scimitar FTS 2000 Fourier transform IR spectrometer (Digilab, Marlborough, MA). Raman spectra of the modified SWCNTs were recorded using a T64000 triple Raman spectrometer (Horiba Jobin Yvon, Milan, Italy). Elemental analysis of the modified SWCNTs was performed using a vario EL cube CHNS analyzer (Abacus Analytical Systems GmbH, Maintal, Germany). Thermogravimetric analysis of the modified SWCNTs was conducted using a TG 209 F1 thermogravimetric analyzer (Netzsch, Hamburg, Germany). The ζ potential was measured using a Nanosizer ZS particle analyzer (Malvern Instruments, Malvern, U.K.). Transmission electron microscopy (TEM) images were obtained using a Veleta digital camera (SIS, Schwentinental/Klausdorf, Germany) mounted on a JEM 1400 transmission electron microscope (JEOL, Japan).

The optical density of the solutions containing the oligonucleotides and their derivatives was measured using a Nanodrop 1000 spectrophotometer (Thermo Fisher Scientific, Waltham, MA). The solutions containing SWCNTs and their hybrids with oligonucleotides were prepared via sonication in a Sonorex Super RK 31 H ultrasonic bath (Bandelin Electronic GmbH & Co. KG, Berlin-Lichterfelde, Germany). The fluorescence spectra were recorded using a Cary Eclipse spectrofluorometer (Varian Inc., Palo Alto, CA) in quartz cuvettes (optical path = 3 mm) at 25 °C. The temperature was maintained using a 2219 Multitemp II thermostatic circulator (LKB, Bromma, Sweden). The mass spectra of the oligonucleotide conjugates were recorded on a matrix-assisted laser desorption ionization time-of-flight (MALDI-TOF) Autoflex Speed mass spectrometer (Bruker Daltonics, Bremen, Germany).

2.4. Functionalization of SWCNTs. Fluorescein-labeled PEGylated SWCNTs were obtained as previously described with modifications.[25,26] SWCNT-COOH (10 mg) was dispersed in 500 μL of deionized water (mQ, Millipore, Billerica, MA) via sonication (35 kHz, 5 min). Then, a solution containing 5 mg of 1-ethyl-3-[3-(dimethylamino)propyl]carbodiimide (EDC; Fluka, St. Louis, MO, 26.2 μmol) in 200 μL of mQ water was added. After stirring (3 h, 25 °C), 15 mg of bis(3-aminopropyl)poly(ethylene glycol) (MW 1500, Aldrich, St. Louis, MO, 10 μmol) in a mixture of 200 μL of mQ water and 10 μL of triethylamine was added, and the reaction mixture was stirred overnight at 25 °C. SWCNT-PEG was precipitated by adding a 10--fold volume of acetone followed by centrifugation (5 min, 14000 g), washed with a mixture of acetone/ethanol/water (90:5:5, v/v; 5 × 2 mL), and dried under vacuum. The primary amino group content was approximately 0.15 mmol/g according to the Kaiser assay.[27]

SWCNT-PEG (10 mg, 1.5 μmol of primary amino groups) was dispersed in a mixture of 200 μL of anhydrous dimethyl sulfoxide (DMSO) and 10 μL of anhydrous triethylamine via sonication (35 kHz, 5 min), and 0.6 mg of fluorescein isothiocyanate (FITC; Fluka, St. Louis, MO, 1.5 μmol) in 200 μL of anhydrous DMSO was added. After stirring (4 h, 45 °C), SWCNT-PEG-FITC was precipitated by the addition of a 10-fold volume of acetone followed by centrifugation (5 min, 14000 g), washed with a mixture of acetone/ethanol (95:5, v/v; 7 × 2 mL), and dried under vacuum.

The functionalized SWCNTs were examined using IR and Raman spectroscopy, fluorescence spectroscopy, elemental analysis, and TGA. The data are provided in the Supporting Information (SI; Tables S-1 and S-2 and Figures S-1−S-6).

2.5. Synthesis of 5′-Pyrene Conjugates of Oligonucleotides. 5′-Pyrene conjugates of oligodeoxyribonucleotides similar to those in ref 28 were obtained. Triphenylphosphine (6.8 mg, 25 μmol) and 2,2′-dipyridyl disulfide (5.3 mg, 25 μmol) in anhydrous DMSO (25 μL each) were added to a solution of 5′-phosphate- or 5′-hexakis(ethylene glycol) phosphate-modified oligonucleotide (cetyltrimethylammonium salt; approximately 0.03 μmol) and 4-(*N*,*N*′-dimethylamino)pyridine (5 mg, 41 μmol) in anhydrous DMSO (50 μL). The reaction mixture was stirred for 15 min at 37 °C. The activated oligonucleotide was precipitated with 2% $LiClO_4$ in acetone, quickly washed with acetone, and dissolved in water (5 μL), followed by the addition of 1-pyrenylmethylamine hydrochloride (0.6 mg, 2.2 μmol) in a DMSO (25 μL)/triethylamine (5 μL) mixture. The reaction mixture was stirred for 2 h at 37 °C. The nucleotide material was precipitated with 2% $LiClO_4$ in acetone and washed with acetone. The obtained conjugates—PyrHEG22, Pyr22, PyrHEG17, and Pyr17—were purified via 15% polyacrylamide gel electrophoresis and their structures confirmed via MALDI-TOF mass spectrometry and UV and fluorescence spectroscopy (for details, see Table S-3 and Figure S-7 in the SI).

2.6. Preparation of Solutions Containing Functionalized SWCNTs and Their Hybrids with Oligonucleotides. To obtain solutions of functionalized SWCNTs with a given pH, SWCNT-COOH, SWCNT-PEG, or SWCNT-PEG-FITC was added to a buffered solution [10 mM sodium cacodylate (pH 5.5, 6.0, 6.5, and 7.0) or 10 mM Tris-HCl (pH 7.5, 8.0, 8.5, and 8.9), 1 mM Na_2EDTA; 0.1 M NaCl] to a final concentration of 0.5−128 mg/L, sonicated for 30 min, and centrifuged (5 min, 14000*g*).

To obtain solutions of the hybrids, functionalized SWCNTs were added to a buffered oligonucleotide solution (10 mM Tris-HCl, pH 7.5; 1 mM Na_2EDTA; 0.1 M NaCl) (1 μM) to a final concentration of 0.5−128 mg/L, sonicated for 30 min, and centrifuged (5 min, 14000*g*).

2.7. Adsorption Isotherms of 5′-Pyrene Conjugates of Oligonucleotides onto SWCNTs. The fluorescence spectra for the noncovalent hybrids of pyrene conjugates of oligonucleotides with functionalized SWCNTs were recorded at λ_{ex} = 345 nm. The oligonucleotide quantity adsorbed onto the SWCNTs, n_{ads}, was calculated using the formula[12] in eq 1

$$n_{ads} = \left(1 - \frac{I_P}{I_P^0}\right) C(\mathrm{Pyr})_\Sigma V \qquad (1)$$

in which I_P is the intensity of the pyrene residue fluorescence at 378 nm in the oligonucleotide−SWCNT hybrid solution, I_P^0 is the intensity of the pyrene residue fluorescence at 378 nm in the reference oligonucleotide solution at the same concentration (1 μM), $C(\mathrm{Pyr})_\Sigma$ is the total concentration of the pyrene-conjugated oligonucleotide (1 μM), and V is the sample volume. This formula does not take into account the possible formation of pyrene excimers that exhibit a fluorescence maximum at 570 nm because the concentration of the pyrene-conjugated oligonucleotides is insufficient for their formation[29] (Figure S-7 in the SI).

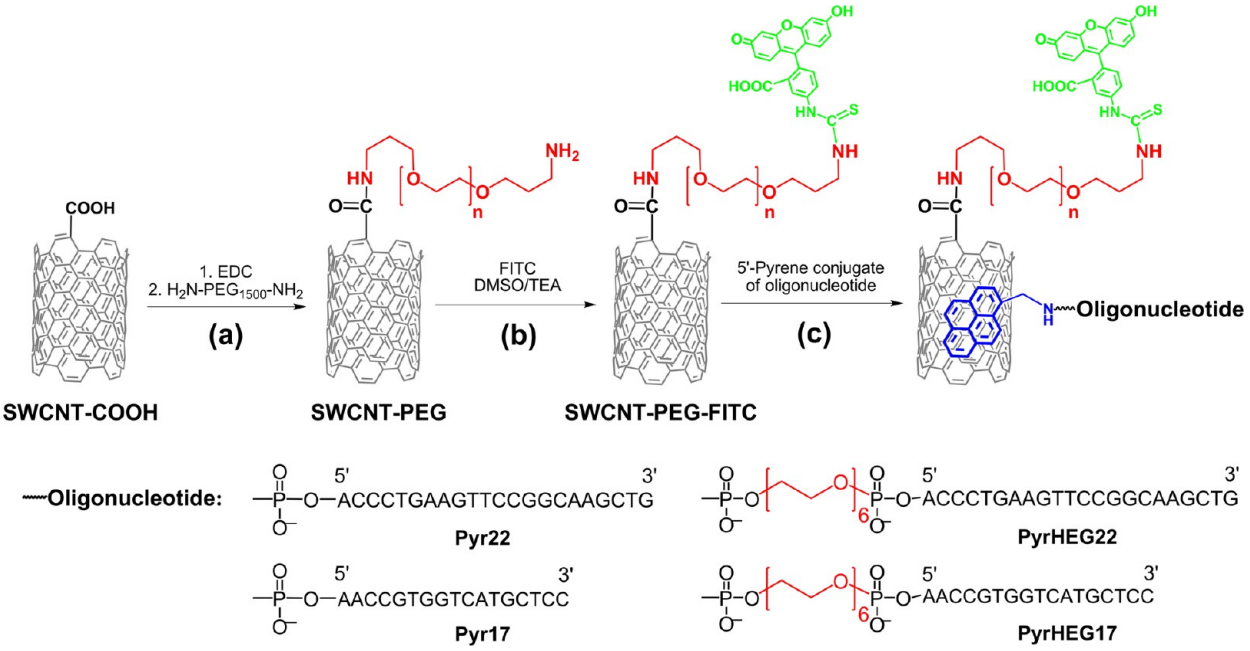

Figure 1. Scheme of the SWCNT multifunctionalization.

2.8. Cytotoxicity Assay. The cytotoxicity of SWCNTs was evaluated using the standard MTT assay.[30] Cells from the KB-3-1, KB-8-5, and HeLa lines were seeded in 96-well plates (3×10^3 cells/well) and cultivated in 100 μL DMEM supplemented with 10% FBS. The cells were incubated at 37 °C in the presence of 5% CO_2 for 24 h. Then, the medium in the wells was replaced with 150 μL of DMEM without serum containing functionalized SWCNTs or their hybrids with oligonucleotides (from 0.001 to 100 mg/L). The cells were incubated with SWCNTs for 4 h; then 150 μL of DMEM with 30% FBS was added, and the cells were incubated for an additional 20 h. After 24 h of incubation in the presence of SWCNTs, MTT was added to the medium to a final concentration of 0.5 mg/L. The absorbance of the samples at 570 nm was measured 3 h after the addition of MTT using a Multiscan RC system (Ani Labsystems, Vantaa, Finland). The data for all experimental points were obtained from four parallel assays. The results are presented as the percentage of living cells relative to the control cells (untreated cells).

2.9. TEM Analysis. *2.9.1. TEM Analysis of the Samples Containing SWCNTs and Their Hybrids with Oligonucleotides.* A drop of aqueous solution containing SWCNTs (3 μL, 25 mg/L) was placed onto a copper grid covered with a Formvar film that was stabilized with carbon and dried at room temperature. The grid was then placed onto a drop of an aqueous solution containing a contrast agent (2% phosphotungstic acid for SWCNT-PEG or 0.5% uranyl acetate for SWCNT-COOH, SWCNT-PEG-FITC, and their hybrids with oligonucleotides) for 5 s. The excess liquid was removed using filter paper. The grids were examined on a JEM 1400 electron microscope (JEOL) operated at an accelerating voltage of 80 kV. The images were collected using a side-mounted Veleta digital camera (SIS, Schwentinental/Klausdorf, Germany).

2.9.2. TEM Analysis of KB-8-5 Cells Exposed to Functionalized SWCNTs and Their Hybrids with Oligonucleotides. The KB-8-5 cells were propagated as described in section 2.8 to obtain confluent monolayers in six-well plates. The cells were then treated with 1 mL SWCNT-COOH, SWCNT-PEG-FITC, or their hybrids with oligonucleotides (10 mg/mL) for 4 h at 37 °C. Untreated KB-8-5 cells served as a control. The cells were collected via trypsin treatment and pelleted at 5000 rpm for 5 min. The pellets were fixed using 4% paraformaldehyde and routinely processed for ultrathin sectioning. The ultrathin sections were prepared using an EM UC7 ultramicrotome (Leica, Wetzlar, Germany), routinely stained with uranyl acetate and lead citrate, and examined on a JEM 1400 transmission electron microscope (JEOL).

3. RESULTS AND DISCUSSION

3.1. Functionalized SWCNTs. Oxidized SWCNTs containing carboxyl groups (SWCNT-COOH) were used as a platform for further functionalization. In the first stage, *O,O′*-bis(3-aminopropyl)PEG_{1500} was attached to SWCNT-COOH using EDC to activate the carboxyl groups (Figure 1a). This method enables the ends and defective sites of SWCNTs to be covalently functionalized, leaving the sidewall unmodified and available for the attachment of nucleic acids. In the second stage, FITC was attached to the terminal amino groups of the PEG moieties (Figure 1b) to form SWCNT-PEG-FITC.

SWCNT functionalization by organic moieties (PEG and FITC) was confirmed by elemental analysis and TGA (Table S-1 and Figure S-1 in the SI) and IR spectroscopy (Table S-2 and Figure S-2 in the SI). The appearance of new bands in the IR spectra corresponding to N−H, C−H, C═O, and C−C bonding vibrations directly indicated functionalization of SWCNTs. D (ω_D = 1230 cm^{-1}) and G (ω_G = 1500−1550 cm^{-1}) bands and the radial breathing mode band (ω_{RBM} = 170 cm^{-1}) corresponding to an SWCNT diameter of 1.3 nm, according to the literature,[31] were observed in the Raman spectra of the functionalized SWCNTs (Figure S-3 in the SI). The I_D/I_G ratio increased because of functionalization.[32]

Although SWCNTs are known as fluorescence quenchers, the presence of a linker between the CNT and fluorescein prevents quenching (examples can be found in the literature[33,34]). The fluorescence intensity of SWCNT-PEG-FITC reached its maximal value at higher pH (8.5−9.0) compared with that of FITC (pH ∼7.5; Figure S-4 in the SI). This shift likely occurs because of a change in the protonation of the fluorescein moieties or shielding after conjugation with SWCNT-PEG.[35] The intensity of the FITC fluorescence maximum at 514 nm (λ_{ex} = 495 nm) at pH 7.5 increased with increasing SWCNT-PEG-FITC concentration up to 50−60 mg/L. A further increase in the SWCNT concentration slightly decreased the fluorescence, likely caused by fluorescence scattering due to formation of the nanotube suspension (Figure S-5 in the SI).

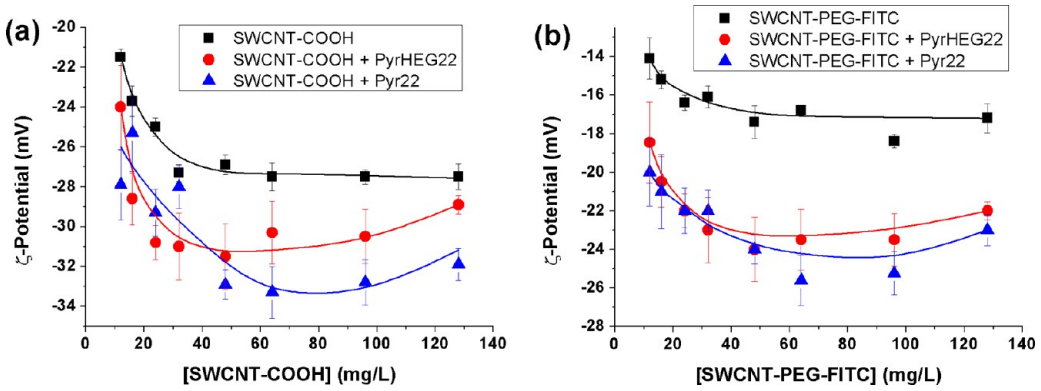

Figure 2. ζ-potential plots for SWCNT-COOH (a) and SWCNT-PEG-FITC (b) and their hybrids with oligonucleotides. Conditions: 10 mM Tris-HCl, 1 mM Na_2EDTA, 0.1 M NaCl, pH 7.5. The oligonucleotide concentration was 1 μM. The data represent the mean values ± standard deviation (n = 5).

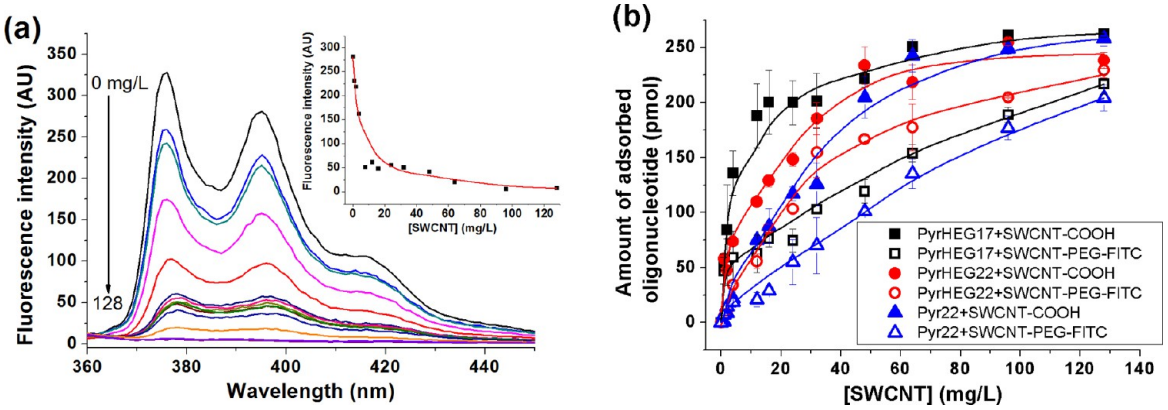

Figure 3. Fluorescence spectra (λ_{ex} = 345 nm) of the hybrid of PyrHEG17 with SWCNT-COOH at SWCNT-COOH concentrations ranging from 0 to 128 mg/L (inset: dependence of the fluorescence intensity at λ_{max} = 378 nm on the SWCNT concentration) (a) and the adsorption isotherms of the pyrene conjugates PyrHEG17, PyrHEG22, and Pyr22 with SWCNT-COOH or SWCNT-PEG-FITC (b) (the data represent the mean values ± standard deviation, n = 3). Conditions: 10 mM Tris-HCl, 1 mM Na_2EDTA, 0.1 M NaCl, pH 7.5, 25 °C. The oligonucleotide concentration was 1 μM.

Functionalized SWCNTs (SWCNT-PEG and SWCNT-PEG-FITC) formed less stable solutions (ζ-potential values of approximately −20 mV) than SWCNT-COOH (−27 mV) at pH values between 5.5 and 8.9 (Figure S-6 in the SI). Nevertheless, the functionalized SWCNTs did not aggregate during several months of storage in solutions containing SWCNT concentrations below 60 mg/L. The subsequent experiments were conducted at pH 7.5.

3.2. 5′-Pyrene Conjugates of Oligonucleotides. The 5′-pyrene model oligodeoxyribonucleotide conjugates Pyr22, PyrHEG22, Pyr17, and PyrHEG17 (Table S-3 in the SI) were synthesized similarly to those in ref 28 by coupling 1-pyrenylmethylamine with the 5′-terminal phosphate group of the oligonucleotide that was selectively activated using triphenylphosphine and 2,2′-dipyridyl disulfide in the presence of 4-(*N*,*N*′-dimethylamino)pyridine as the nucleophilic catalyst.[36,37] The pyrene residues were conjugated with the oligonucleotides via a phosphamide bond. The hexakis-(ethylene glycol) linker provided the conformational mobility in the pyrene residue, thus facilitating its interaction with SWCNTs.

3.3. Hybrids of SWCNTs with Oligonucleotides. The pyrene conjugates of 5′-phosphate- or 5′-hexakis(ethylene glycol) phosphate-modified oligodeoxyribonucleotides were noncovalently attached to SWCNT-COOH and SWCNT-PEG-FITC (Figure 1c). The pyrene residues were adsorbed onto the defect-free sites of the SWCNT surface, thus anchoring the oligonucleotide. This process was performed under relatively mild conditions (short-term sonication), with the oligonucleotides remaining stable and undamaged.[22]

A comparative study of immobilization of the 5′-pyrene conjugates of oligonucleotides onto the SWCNT-COOH and SWCNT-PEG-FITC surfaces was performed to evaluate the effect of the functional groups on oligonucleotide adsorption and to determine the conditions of maximum oligonucleotide loading on the modified SWCNTs.

The effect of the oligonucleotides on the hydrodynamic properties of the functionalized SWCNTs was examined via ζ-potential measurements at an SWCNT concentration of 12−128 mg/L. The plots of the ζ potentials exhibited minima at the points believed to correspond to the maximal quantity of oligonucleotide adsorbed onto individual SWCNTs (Figure 2).

The efficiency of oligonucleotide adsorption onto the SWCNT-COOH and SWCNT-PEG-FITC surfaces was assessed via fluorescence titration of the solutions containing the pyrene-conjugated oligonucleotides with SWCNTs at concentrations ranging from 0.5 to 128 mg/L (Figure 3). The fluorescence intensity decreased with increasing SWCNT concentration because of the fluorescence quenching of pyrene upon its adsorption onto SWCNTs.[23] The quantity of

dx.doi.org/10.1021/am4034729 | ACS Appl. Mater. Interfaces 2014, 6, 1454−1461

conjugates adsorbed was calculated from the fluorescence quenching data. The capacity of SWCNTs for oligonucleotide adsorption was calculated by analogy with ref 12. The attachment of large functional groups (such as PEG) to SWCNTs was shown to hinder the adsorption of pyrene conjugates of oligonucleotides. The introduction of a hexakis-(ethylene glycol) linker into the oligonucleotide structure slightly facilitated this adsorption, which can be explained by the increased conformational mobility of the pyrene residue. The increased oligonucleotide length negatively impacted the adsorption efficiency of the pyrene residues, likely because of stacking interactions between the heterocyclic bases of the oligonucleotides and the SWCNT surface. The SWCNT capacity was 20−100 μmol/g oligonucleotide depending on the conjugate structure and the type of SWCNT functionalization. The SWCNT/oligonucleotide ratios that resulted in both the minima in the ζ-potential plots (Figure 2) and the plateaus in the adsorption isotherm plots were considered optimal for forming hybrids (Figure 3b).

3.4. TEM Study of the Functionalized SWCNTs and Their Hybrids with Oligonucleotides. The morphology of the modified SWCNTs and their hybrids with oligonucleotides prepared under the optimal conditions was examined using TEM after staining with phosphotungstic acid or uranyl acetate. The use of contrast agents permitted visualization of the charged functional groups (PEG and PEG-FITC) and oligonucleotides on the SWCNT surface under relatively low magnification (Figure 4). Visualization was achieved because of either the electrostatic interactions between the uranyl cations and both the carboxyl groups of FITC and the phosphate groups of the oligonucleotide backbone or the interaction between the tungstate anions and the free terminal amino groups of PEG.

Bundles of SWCNTs with diameters of 10−20 nm and lengths of up to 1 μm were observed in the electron micrographs. After contrast enhancement, the attachment sites of the organic functional groups on the SWCNT surface were observed as electron-dense spots on the nanotube surface (white arrows in Figure 4b,c,e). After staining, the oligonucleotide adsorption sites appeared as rounded structures with a diameter of approximately 5 nm on the surface of the nanotubes. In the absence of a contrast agent, no electron-dense structures were observed on the SWCNT surface.

3.5. Cytotoxicity Studies. Although broad studies have been conducted regarding the cytotoxicity of CNTs themselves (examples can be found in the literature[38,39]), the effect of SWCNT functionalization on the CNT toxicity is a topic of intense investigation.[40,41] A comparative study between the cytotoxicity of the modified SWCNTs and that of their hybrids was necessary to determine the role of different potentially bioactive functionalities (SWCNTs, pyrene, and oligonucleotides) in cytotoxicity.

The cytotoxicity of the modified SWCNTs toward HeLa, KB-3-1, and KB-8-5 cells was evaluated using the MTT assay[30] (Figure 5). The dose-response toxicity of all studied SWCNTs and their hybrids with oligonucleotides was revealed. The results demonstrated that the cell lines displayed different levels of sensitivity to the modified SWCNTs, with HeLa cells exhibiting the lowest sensitivity and KB-3-1 cells exhibiting the greatest sensitivity; the IC_{50} values for the KB-3-1 cells were 4.3 and 19.3 mg/L for SWCNT-COOH (Figure 5a) and SWCNT-PEG-FITC (Figure 5b), respectively. In general, the PEGylation of SWCNTs increased their biocompatibility,

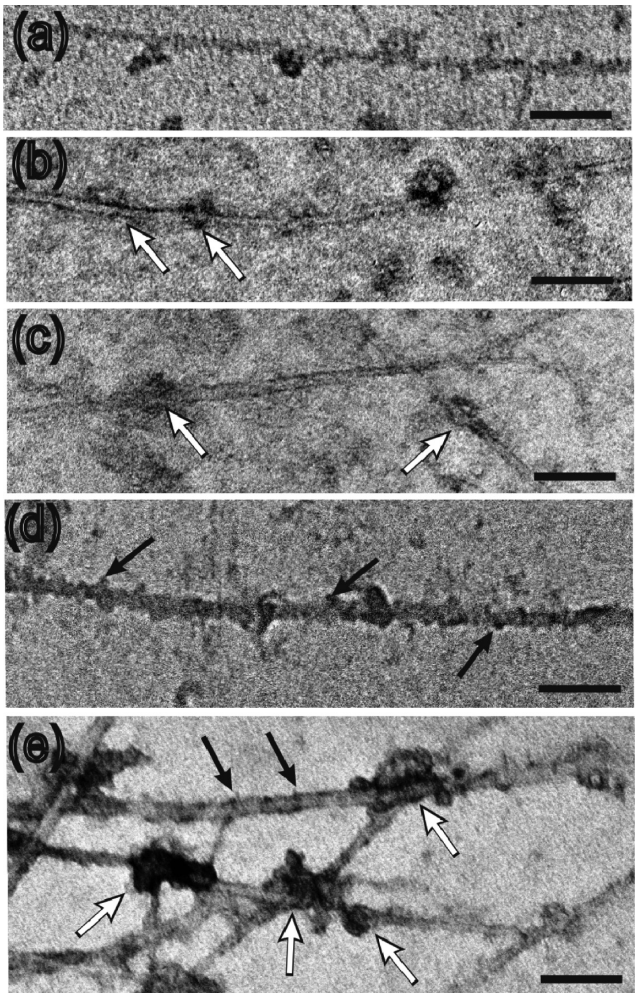

Figure 4. TEM images of SWCNT-COOH (a), SWCNT-PEG (b), SWCNT-PEG-FITC (c), hybrid of SWCNT-COOH with PyrHEG17 (d), and hybrid of SWCNT-PEG-FITC with PyrHEG17 (e). The white arrows indicate the sites of SWCNT functionalization; the black arrows indicate the sites of oligonucleotide adsorption onto the SWCNT surface. The samples were stained with uranyl acetate (a and c−e) or phosphotungstic acid (b). The scale bar corresponds to 100 nm.

which is in agreement with the literature data.[9,10] The data for the HeLa, KB-3-1, and KB-8-5 cell viability after exposure to the functionalized SWCNTs are similar to those obtained using other cell cultures.[42−45] Certain variations in the cell viability could be explained by particular features of the cell lines[46] or by the SWCNT morphology.[6] The unusual deviation from the dose-response behavior at high SWCNT concentrations (Figure 5a) can be explained by the partial aggregation of highly concentrated SWCNTs with the cells, which may have utilized these aggregates as substrates for growth.[47,48]

The effect on cytotoxicity of immobilizing an oligonucleotide on the surface of modified SWCNTs was evaluated using KB-8-5 cells and hybrids of PyrHEG17 with SWCNT-COOH or SWCNT-PEG-FITC. This oligonucleotide was chosen for biological testing because it is not complementary to any sequence in the human genome,[49] thereby eliminating any effects on the cell viability of the biological activity of oligonucleotides attached to SWCNTs. The IC_{50} values for the SWCNT-oligonucleotide hybrids were not achieved even at hybrid concentrations of 100 mg/L (Figure 5c), exhibiting

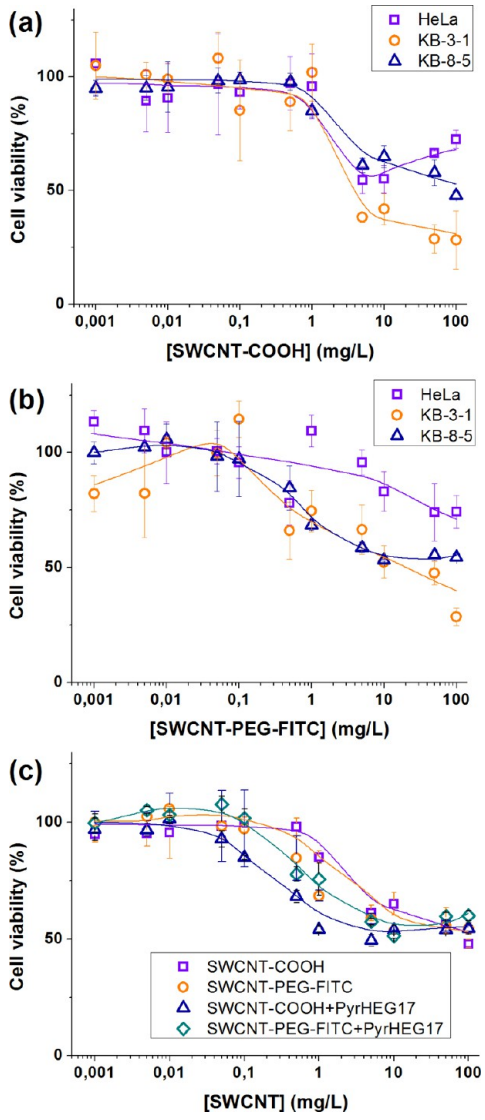

Figure 5. Viability of HeLa, KB-3-1, and KB-8-5 cells treated with SWCNT-COOH (a) or SWCNT-PEG-FITC (b). Viability of KB-8-5 cells treated with SWCNT-COOH, SWCNT-PEG-FITC, or their hybrids with PyrHEG17 (c). The data represent the mean values ± standard deviation (n = 4).

smaller toxicity in comparison with previously reported hybrids.[50] The results obtained demonstrate that the functionalized SWCNTs and their oligonucleotide hybrids possess low toxicity and can be used in biological systems.

3.6. Ultrastructural Characterization of the Interaction between Functionalized SWCNTs and KB-8-5 Cells. An ultrastructural examination of the cells treated with functionalized SWCNTs or their hybrids with oligonucleotides was performed to confirm that the nanotubes had interacted with the cells. The morphology of KB-8-5 cells treated with modified SWCNTs was compared with that of untreated cells.

Treating the KB-8-5 cells with modified SWCNTs caused no visible morphological damage (Figure 6). The cells in both the experimental and untreated cultures had large nuclei with high euchromatin content and one or two well-developed nucleoli. The cytoplasm contained oval mitochondria, large quantities of free ribosomes, a few cisternae of endoplasmic reticulum, and a relatively small Golgi complex. Few endosomes and lysosomes were observed. Mitotic cells were observed in all samples of

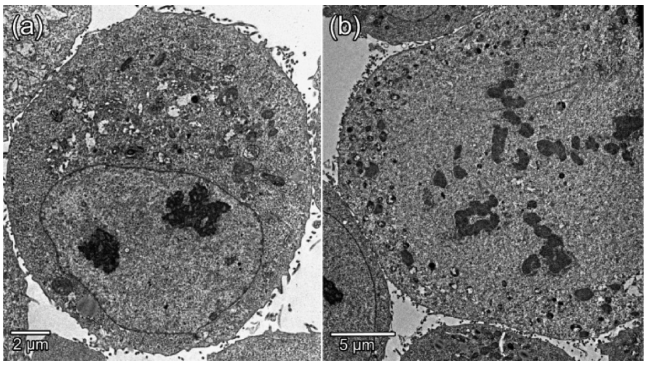

Figure 6. KB-8-5 cells after 4 h treatment with hybrids of SWCNT-PEG-FITC and PyrHEG17: (a) image of a cell with a large nucleus and two prominent nucleoli; (b) image of a dividing cell with mitotic chromosomes. The images were obtained on a JEM 1400 transmission electron microscope (JEOL) operated at an an accelerating voltage of 80 kV.

KB-8-5 cells treated with the modified SWCNTs, which demonstrated the low genotoxicity of these SWCNTs.

Obviously, individual nanotubes with a thickness of approximately 1 nm cannot be seen in ultrathin sections that are 60−80 nm thick; thus, only bundles of nanotubes by TEM were observed. Most of the bundles of modified SWCNTs had diameters of 5−10 nm and were observed together with amorphous carbon nanoparticles in the ultrathin sections (Figure 7).

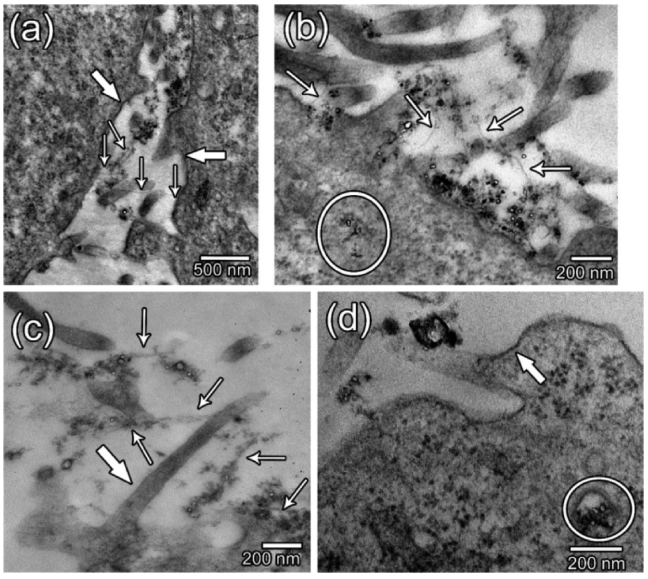

Figure 7. TEM images of KB-8-5 cells exposed to SWCNTs and their hybrids with oligonucleotides: (a) hybrid of SWCNT-COOH with PyrHEG17 between two cells; (b−d) functionalized SWCNTs adsorbed onto the surface of a cell and onto cellular protrusions. Bundles of nanotubes are indicated by the thin arrows; the cellular plasma membrane is indicated by the thick arrows. The black particles colocalized with the nanotubes are likely amorphous carbon nanoparticles. The rings indicate endocytotic vesicles containing SWCNTs. Treatment with (a) a hybrid of SWCNT-COOH with PyrHEG17, (b) SWCNT-COOH, (c) SWCNT-PEG-FITC, and (d) a hybrid of SWCNT-PEG-FITC with PyrHEG17. The images were obtained using a JEM 1400 transmission electron microscope (JEOL) operated at an accelerating voltage of 80 kV.

dx.doi.org/10.1021/am4034729 | ACS Appl. Mater. Interfaces 2014, 6, 1454−1461

Modified SWCNTs adsorbed onto the cellular surfaces and protrusions were observed in all samples. The KB-8-5 cells in contact with the nanotubes exhibited no signs of cytoplasmic alteration in the areas adjacent to the nanotube adsorption sites or in other regions of the cytoplasm. Nanotubes absorbed onto cells were more frequently observed in the KB-8-5 cells treated with SWCNT-COOH or hybrids with oligonucleotides, whereas the presence of PEG reduced the ability of the nanotubes to adsorb onto the cell membrane. Some of the KB-8-5 cells incubated with SWCNT-COOH or their hybrids with oligonucleotides possessed carbon nanoparticles in their endocytotic vesicles and endosomes.

The TEM study demonstrated that the absorption of functionalized SWCNTs and their hybrids onto KB-8-5 cells did not affect the cell morphology or block mitotic division during the 4 h incubation. SWCNTs interacted with the cell membrane and could be internalized by a cell without visible damage to the cellular structures.

4. CONCLUSIONS

Novel multifunctional hybrids of nucleic acids and CNTs were designed. Oxidized SWCNTs were covalently functionalized at the tips and defective sites using diaminopoly(ehtylene glycol)and fluorescein, consecutively. The pyrene residues that were attached to the 5′-termini of the oligonucleotides via linkers of varying lengths were used as the anchor groups for immobilizing oligonucleotides on the nonfunctionalized sites of the SWCNT surface. The formation of noncovalent hybrids of functionalized SWCNTs with the pyrene conjugates of the oligodeoxyribonucleotides was demonstrated. Both the functionalized SWCNTs and their hybrids with oligonucleotides were characterized using physicochemical methods. The low toxicity and effective interaction of the modified SWCNTs and their hybrids with cells renders them potential nanotransporters. Because these modified SWCNTs are suitable for attaching different oligonucleotides, the approach demonstrated herein allows for the rational design of multifunctional CNT-based constructs as platforms for future nucleic acid therapeutics and diagnostics.

■ ASSOCIATED CONTENT

Supporting Information

Details on the characterization of functionalized SWCNTs and pyrene conjugates of oligonucleotides. This material is available free of charge via the Internet at http://pubs.acs.org.

■ AUTHOR INFORMATION

Corresponding Author

*E-mail: eka@niboch.nsc.ru.

Author Contributions

The manuscript was written through the contributions of all authors. All authors have given approval to the final version of the manuscript.

Notes

The authors declare no competing financial interest.

■ ACKNOWLEDGMENTS

The authors are grateful to Dr. M. A. Vorobjeva (ICBFM SB RAS) for synthesis of the oligonucleotides and Dr. V. A. Volodin (ISP SB RAS, NSU), Dr. L. A. Sheludyakova (NIIC SB RAS), and the Centre of Collective Use "Nanostructures" of the SB RAS for analysis of the SWCNTs. This work was supported by RFBR Grant 14-03-31691, RFBR-CNRS Grant 12-04-91053, a grant from the Ministry of Education and Science of Russian Federation (Grant 8739), the RAS Presidium Programme 4, a grant of the Government of Russian Federation for support of scientific research projects implemented under the supervision of the world's leading scientists (Agreement 14.B25.31.0028), a FASIE grant, and the Scholarship of the President of the Russian Federation (Grant 6266.2013.4).

■ REFERENCES

(1) Eder, D. *Chem. Rev.* **2010**, *110*, 1348−1385.
(2) Tasis, D.; Tagmatarchis, N.; Bianco, A.; Prato, M. *Chem. Rev.* **2006**, *106*, 1105−1136.
(3) Cui, D. *J. Nanosci. Nanotechnol.* **2007**, *7*, 1298−1314.
(4) Foldvari, M.; Bagonluri, M. *Nanomedicine (N. Y., NY, U. S.)* **2008**, *4*, 173−182.
(5) Foldvari, M.; Bagonluri, M. *Nanomedicine (N. Y., NY, U. S.)* **2008**, *4*, 183−200.
(6) Vashist, S. K.; Zheng, D.; Pastorin, G.; Al-Rubeaan, K.; Luong, J. H. T.; Sheu, F.-S. *Carbon* **2011**, *49*, 4077−4097.
(7) Wei, W.; Sethuraman, A.; Jin, C.; Monteiro-Riviere, N. A.; Narayan, R. J. *J. Nanosci. Nanotechnol.* **2007**, *7*, 1284−1297.
(8) Bianco, A.; Kostarelos, K.; Prato, M. *Curr. Opin. Chem. Biol.* **2005**, *9*, 674−679.
(9) Bottini, M.; Rosato, N.; Bottini, N. *Biomacromolecules* **2011**, *12*, 3381−3393.
(10) Ravelli, D.; Merli, D.; Quartarone, E.; Profumo, A.; Mustarelli, P.; Fagnoni, M. *RSC Adv.* **2013**, *3*, 13569−13582.
(11) Kelkar, S. S.; Reineke, T. M. *Bioconjugate Chem.* **2011**, *22*, 1879−1903.
(12) Apartsin, E. K.; Buyanova, M. Y.; Novopashina, D. S.; Ryabchikova, E. I.; Venyaminova, A. G. In *Nanomaterials Imaging Techniques, Surface Studies, and Applications*; Fesenko, O., Yatsenko, L., Brodin, M., Eds.; Springer Proceedings in Physics; Springer Science + Business Media: New York, 2013; Vol. *146*, pp 291−307.
(13) Kam, N. W.; Liu, Z.; Dai, H. *J. Am. Chem. Soc.* **2005**, *127*, 12492−12493.
(14) Liu, Z.; Winters, M.; Holodniy, M.; Dai, H. *Angew. Chem., Int. Ed.* **2007**, *46*, 2023−2027.
(15) Liu, Z.; Tabakman, S. M.; Chen, Z.; Dai, H. *Nat. Protocols* **2009**, *4*, 1372−1382.
(16) Liu, Z.; Robinson, J. T.; Tabakman, S. M.; Yang, K.; Dai, H. *Mater. Today* **2011**, *14*, 316−323.
(17) Taft, B. J.; Lazareck, A. D.; Withey, G. D.; Yin, A.; Xu, J. M.; Kelley, S. O. *J. Am. Chem. Soc.* **2004**, *126*, 12750−12751.
(18) Baek, Y.-K.; Jung, D.-H.; Yoo, S. M.; Shin, S.; Kim, J.-H.; Jeon, H.-J.; Choi, Y.-K.; Lee, S. Y.; Jung, H.-T. *J. Nanosci. Nanotechnol.* **2011**, *11*, 4210−4216.
(19) Apartsin, E. K.; Novopashina, D. S.; Nastaushev, Yu. V.; Venyaminova, A. G. *Nanotechnol. Russ.* **2012**, *7*, 99−109.
(20) Wu, W.; Wieckowski, S.; Pastorin, G.; Benincasa, M.; Klumpp, C.; Briand, J.-P.; Gennaro, R.; Prato, M.; Bianco, A. *Angew. Chem., Int. Ed.* **2005**, *44*, 6358−6362.
(21) Boutorine, A. S.; Le Doan, T.; Battioni, J. P.; Mansuy, D.; Dupre, D.; Helene, C. *Bioconjugate Chem.* **1990**, *1*, 350−356.
(22) Novopashina, D. S.; Apartsin, E. K.; Venyaminova, A. G. *Ukr. J. Phys.* **2012**, *57*, 718−722.
(23) Wang, L.; Zhang, L.; Xue, X.; Geb, G.; Liang, X. *Nanoscale* **2012**, *4*, 3983−3989.
(24) Novopashina, D. S.; Sinyakov, A. N.; Ryabinin, V. A.; Venyaminova, A. G.; Halby, L.; Sun, J.-S.; Boutorine, A. S. *Chem. Biodiversity* **2005**, *2*, 936−952.
(25) Cheng, J.; Fernando, K. A. S.; Veca, L. M.; Sun, Y.-P.; Lamond, A. I.; Lam, Y. W.; Cheng, S. H. *ACS Nano* **2008**, *2*, 2085−2094.
(26) Huang, W.; Fernando, S.; Allard, L. F.; Sun, Y.-P. *Nano Lett.* **2003**, *3*, 565−568.

(27) Sarin, V. K.; Kent, S. B.; Tam, J. P.; Merrifield, R. B. *Anal. Biochem.* **1981**, *117*, 147−157.
(28) Novopashina, D. S.; Totskaya, O. S.; Kholodar, S. A.; Meshchaninova, M. I.; Venyaminova, A. G. *Russ. J. Bioorg. Chem.* **2008**, *34*, 602−612.
(29) Winnik, F. M. *Chem. Rev.* **1993**, *93*, 587−614.
(30) Carmichael, J.; DeGraff, W. G.; Gazdar, A. F.; Minna, J. D.; Mitchell, J. B. *Cancer Res.* **1987**, *47*, 936−942.
(31) Thomsen, C.; Reich, S. In *Light Scattering in Solid IX*; Cardona, M., Merlin, R., Eds.; Springer: Berlin, 2007; Vol. *108*, pp 115−234.
(32) Andrada, D. M.; Vieira, H. S.; Oliveira, M. M.; Santos, A. P.; Yin, L.; Saito, R.; Pimenta, M. A.; Fantini, C.; Furtado, C. A. *Carbon* **2013**, *56*, 235−242.
(33) Pantarotto, D.; Briand, J.-P. P.; Prato, M.; Bianco, A. *Chem. Commun.* **2004**, *40*, 16−17.
(34) Nakayama-Ratchford, N.; Bangsaruntip, S.; Sun, X.; Welsher, K.; Dai, H. *J. Am. Chem. Soc.* **2007**, *129*, 2448−2449.
(35) Sjoback, R.; Nygren, J.; Kubista, M. *Spectrochim. Acta, Part A* **1995**, *51*, L7−L21.
(36) Zarytova, V.; Ivanova, E.; Venyaminova, A. *Nucleosides Nucleotides* **1998**, *17*, 649−662.
(37) Zarytova, V. F.; Godovikova, T. S.; Kutyavin, I. V; Khalimskaya, L. M. In *Biophosphates and their analogues, synthesis, structure, metabolism and activity*; Bruzik, K. S., Stec, W. S., Eds.; Elsevier: Amsterdam, The Netherlands, 1987; pp 149−164.
(38) Firme, C. P.; Bandaru, P. R. *Nanomedicine (N. Y., NY, U. S.)* **2010**, *6*, 245−256.
(39) Yang, S.-T.; Luo, J.; Zhou, Q.; Wang, H. *Theranostics* **2012**, *2*, 271−282.
(40) Pan, B.; Cui, D.; Xu, P.; Chen, H.; Liu, F.; Li, Q.; Huang, T.; You, X.; Shao, J.; Bao, C.; Gao, F.; He, R.; Shu, M.; Ma, Y. *Chin. J. Cancer Res.* **2007**, *19*, 1−6.
(41) Ahmed, M.; Jiang, X.; Deng, Z.; Narain, R. *Bioconjugate Chem.* **2009**, *20*, 2017−2022.
(42) Wörle-Knirsch, J. M.; Pulskamp, K.; Krug, H. F. *Nano Lett.* **2006**, *6*, 1261−1268.
(43) Zhang, Y.; Xu, Y.; Li, Z.; Chen, T.; Lantz, S. M.; Howard, P. C.; Paule, M. G.; Slikker, W.; Watanabe, F.; Mustafa, T.; Biris, A. S.; Ali, S. F. *ACS Nano* **2011**, *5*, 7020−7033.
(44) Zhang, T.; Tang, M.; Kong, L.; Li, H.; Zhang, T.; Zhang, S.; Xue, Y.; Pu, Y. *J. Hazard. Mater.* **2012**, *219-220*, 203−212.
(45) Ma, X.; Zhang, L.-H.; Wang, L.-R.; Xue, X.; Sun, J.-H.; Wu, Y.; Zou, G.; Wu, X.; Wang, P. C.; Wamer, W. G.; Yin, J.-J.; Zheng, K.; Liang, X.-J. *ACS Nano* **2012**, *6*, 10486−10496.
(46) Magrez, A.; Kasas, S.; Salicio, V.; Pasquier, N.; Seo, J. W.; Celio, M.; Catsicas, S.; Schwaller, B.; Forro, L. *Nano Lett.* **2006**, *6*, 1121−1125.
(47) Kalbacova, M.; Broz, A.; Kromka, A.; Babchenko, O.; Kalbac, M. *Carbon* **2011**, *49*, 2926−2934.
(48) Baik, K. Y.; Park, S. Y.; Heo, K.; Lee, K.-B.; Hong, S. *Small* **2011**, *7*, 741−745.
(49) Zhang, K.; Wang, Q.; Xie, Y.; Mor, G.; Sega, E.; Low, P. S.; Huang, Y. *RNA* **2008**, *14*, 577−583.
(50) Lu, Q.; Moore, J. M.; Huang, G.; Mount, A. S.; Rao, A. M.; Larcom, L. L.; Ke, P. C. *Nano Lett.* **2004**, *4*, 2473−2477.